Available online at www.CivileJournal.org

Civil Engineering Journal

(E-ISSN: 2476-3055; ISSN: 2676-6957)

Vol. 12, No. 01, January, 2026

Spatial Prediction of Soil Index Properties Using GIS and Empirical Bayesian Kriging

Waseem H. Al-Baghdadi [1], Sohaib K. Al-Mamoori [1*], Laheab A. Al-Maliki [2]

[1] *Department of Civil Engineering, Faculty of Engineering, University of Kufa, Najaf, Iraq.*

[2] *Department of Hydraulic Structures and Water Resources, Faculty of Engineering, University of Kufa, Najaf, Iraq.*

Received 29 September 2025; Revised 01 December 2025; Accepted 09 December 2025; Published 01 January 2026

Abstract

The purpose of this study is to assess the possible use of Empirical Bayesian Kriging (EBK) combined with Geographic Information Systems (GIS) to map and analyze geotechnical index properties in Thi Qar Province in southern Iraq. The aim of this objective is to describe the spatial variability of soil limits of the consistency and define areas with expansive soils, which may influence infrastructure development. Data on 550 boreholes and 862 observations per soil property, including Liquid Limit (LL), Plastic Limit (PL), and Plasticity Index (PI), were analyzed. To test the predictive accuracy of the EBK model and thus assure its statistical validation, RMSE, MSD, RMSSD, and correlation coefficients were used to test the model. The findings show that the LL was between 32% and 69%, the PL between 9% and 36%, and the PI between 1% and 39%, with most of the soils being CL and CH, which signifies moderate-high plasticity. The results indicate that there are good spatial patterns, and plasticity is more dense in the north and central areas. The originality of this work is the use of EBK to create detailed digital soil maps of a semi-arid area, where the available geotechnical data is sparse, which is used to form a dependable base to support engineering design, land-use planning, and regional geotechnical modelling.

Keywords: Geotechnical Mapping; GIS; EBK; Soil Index Properties; Digital Soil Maps; Spatial Interpolation; Soil Classification.

1. Introduction

Atterberg limits and soil index properties especially are some of the most important parameters in geotechnical engineering [1]. These limits establish the limits between liquid, plastic, and semi-solid states of fine-grained soils that define the mechanical behavior, compressibility, shear strength, and permeability of the soils [2]. Proper understanding of the spatial distribution of these properties is essential to the design of important infrastructure, such as foundation design, roadways, earth dam stability analysis, and evaluation of liquefaction potential [3]. Conventional geotechnical studies are based on discrete borehole sampling, having very narrow data points. Nevertheless, high-resolution maps updated continuously have to be used to plan effectively at the regional level and large-scale engineering projects that also take into account the natural spatial variability of soil property within a specific area [4].

Geostatistical methods incorporated into Geographic Information Systems (GIS) often form the basis of the transition between discrete point data and continuous spatial surfaces [5]. Of these approaches, Kriging is known to be widely used due to its ability to provide the Best Linear Unbiased Prediction (BLUP) of spatially related variables, which provides both prediction estimates and the confidence measures of these predictions [6]. Many studies have effectively used Kriging to map various underground conditions such as soil moisture content, soil density, and the

* Corresponding author: sohaib.almamoori@uokufa.edu.iq

https://doi.org/10.28991/CEJ-2026-012-01-07

concentration of contaminants in their environment and agriculture, thus showing the effectiveness of the technique in environmental and agricultural applications [7, 8]. In more recent work, these methods are being taken to critical geotechnical parameters, with Ordinary Kriging (OK) and Universal Kriging (UK) being used to simulate the spatial variability of Atterberg limits and standard penetration test (SPT) values under different urban and regional conditions globally [9, 10].

Although traditional Kriging techniques are powerful in terms of spatial predictions, they are often stationary-based and may require complex manual variogram modelling, which is subject to biasing, especially in the case of dealing with large and geologically diverse areas [11]. In places with complicated alluvial formations and non-steady shifts, e.g., the Mesopotamian plain in Southern Iraq, more cutting-edge geostatistical techniques are obligatory to improve predictability and reduce uncertainty more effectively [12]. Although there is an acute requirement to provide quality geotechnical data that will support a high pace of infrastructure development in the area, high-resolution spatial mapping of the important index properties (LL and PI) in Thi Qar Governorate remains conspicuously missing in the published literature [13]. The available regional data tends to be limited or contains crude methods of interpolation and thus does not reflect the complex, localized variability necessary to modern-day engineering design and risk analysis [14]. This gap highlights the importance of an advanced, information-swerving strategy that would reduce the subjectivity of modeling options as much as possible and maximize predictability.

Recent developments have prompted the use of three-dimensional Empirical Bayesian Kriging (EBK) constructs in geotechnical spatial models (e.g., Utepov et al. [15]; Viegas et al. [16, 17]) and the combination of Geographic Information Systems (GIS) and machine-learning methods (Tzampoglou et al. [18]). There are also methodologies that are being developed to handle non-stationary soil data [19]. Nevertheless, the EBK use in mapping the soil index properties in semi-arid provinces willing to map properties in southern Iraq, among others, is lacking.

To address this significant data and methodological gap, the current study uses the Empirical Bayesian Kriging (EBK) algorithm, within a GIS framework, to produce the most accurate spatial prediction maps of the Liquid Limit, Plastic Limit and Plasticity Index throughout the Thi Qar Governorate. EBK also addresses the limitations of the conventional Kriging by automating the variogram estimation process and incorporating local uncertainty with simulation, which generates more reliable and robust predictions [20]. The main aims of the investigation reported in this paper include: (1) completing a systematic review of a large database of available borehole data; (2) modeling and confirming the EBK model to predict the spatial distribution of LL, PL, and PI; and (3) generating the basic engineering maps that will form a starting point in geotechnical design and regional development planning in Southern Iraq. This study therefore largely contributes substantively by implementing an advanced geostatistical methodology to a data-poor, geotechnically problematic area, hence setting a new standard of spatial geotechnical modeling in the Middle East. In addition to that, the theoretical approach is discussed in detail, and a workflow diagram is provided to make it reproducible and understandable.

The rest of the paper will be structured as follows. Section 2 defines the area of study and gives the data that is used in the spatial analysis. The approach to methodology has been presented in section 3, which gives the laboratory testing processes and Empirical Bayesian Kriging (EBK) interpolation technique. Section 4 presents and discusses the spatial distribution results for the Liquid Limit (LL), Plastic Limit (PL), and Plasticity Index (PI). Section 5 discusses the influence of geological, climatic, and depth-related factors on soil variability. Finally, Section 6 concludes the study by summarizing the main findings, highlighting the practical implications, and suggesting future research directions.

2. Description of Study Area

Thi Qar Governorate, located in southern Iraq (see Figure 1), spans approximately 13,839 km², comprising about 3% of the country's area [21]. It is bordered by five provinces and characterized by a desert climate, with extreme temperatures exceeding 51°C during summer. The annual rainfall averages between 100 mm and 180 mm. The main water sources include the Euphrates River and the Al-Gharraf stream [22].

2.1. Spatial Analysis of Index Properties

The study considers index properties of soils that are expressed by the liquid limit, plastic limit, liquidity index, and plasticity index. The soil was discarded into layers with a 2 m thickness and a total depth of 0-20 m. The primary data were obtained through field investigation reports. Table 1 shows borehole numbers and data used in each characteristic.

Table 1. Information About the Data Used in This Study

No.	Property	Boreholes No.	Data No.
1	Liquid Limit (LL)	550	862
2	Plastic Limit (PL)	550	862
3	Plasticity Index (PI)	550	862
4	Liquidity Index (LI)	550	862

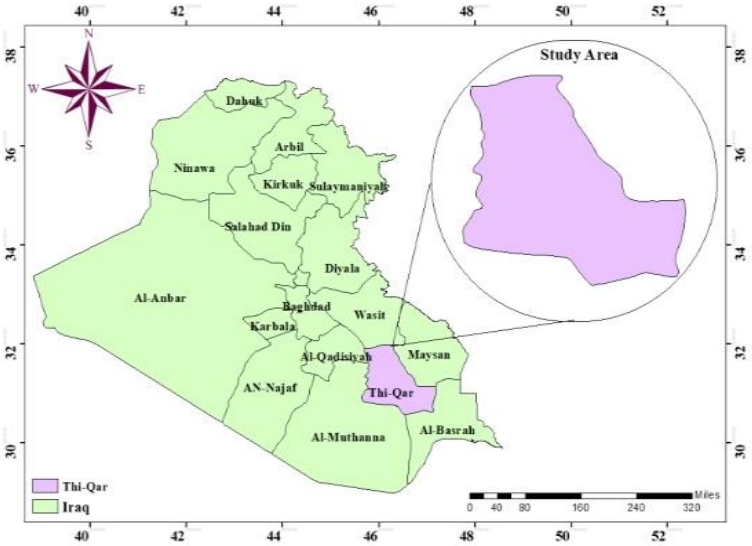

Figure 1. Study Area Location Map

3. Methodology

The research used a sample of 550 of the boreholes whose location is spread throughout the province. ASTM standards were used to have the soil samples analyzed in accredited laboratories. The model consisted of ten 2-meter-thick layers, with an overall depth of 20 meters. Sieve and hydrometer determination using ASTM D6913 was used to characterize particle-size distribution.

The EBK method was used in spatial interpolation due to its ability to consider variogram-parameter uncertainty. To verify the reliability of the results, statistical validation was done using RMSE, MSD, RMSSD, and correlation coefficients.

3.1. Data Collection

A detailed subsurface geological database was prepared in Thi-Qar Governorate, where 550 different borehole logs were included. The purchase of such logs is one of the components of a complex data-collection approach that was used in this study. The positions of the borehole sites are important to the spatial distribution, just as is the accuracy of the borehole sites' positions. The sites of the boreholes were mapped to determine distribution (Figure 2). Unsuitable borehole logs would later be filtered out of the dataset.

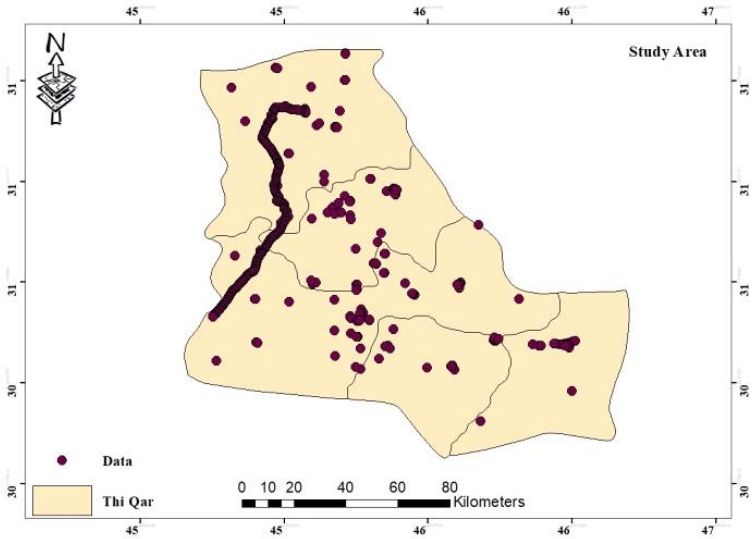

Figure 2. A Base Map of Borehole Locations

3.2. Test methods

The soil samples were extruded, tested, and reported by Thi Qar University Laboratory and the Multidisciplinary Laboratory, and all the tests were performed according to ASTM standards.

3.3. Particle Size Distribution (ASTM D 6913)

The distribution of soil particle sizes was determined for the field soils using both sieve analysis and hydrometer analysis.

3.4. Atterberg limits

Originally, Albert Atterberg defined six "limits of consistency" to characterize the behavior of fine-grained soils: the liquid limit, the plastic limit, the cohesion limit, and the shrinkage limit. Contemporary geotechnical engineering practice, however, typically employs the term "Atterberg Limits" to refer specifically to the liquid limit, plastic limit, and shrinkage limit. The liquid limit and plastic limit are commonly determined through laboratory testing of soil samples, as outlined in ASTM D 4318. Atterberg limit tests are among the most frequently specified by geotechnical engineers in practice [23].

3.4.1. Soil Classification and Identification

Since expansive soil has become a significant issue for engineering projects, there has been a rapid increase in the study of expansive soil, and there are now countless studies regarding expansive soil published every year all over the world. Many different techniques are suggested in these papers by researchers for recognizing and categorizing expansive soil and its swelling potential. Atterberg limits: Qusai et al. (2025) demonstrated that the plasticity index is one of the best metrics for determining how various clays will swell [24]. Extensive soil categorization systems are devised in response to the challenges they bring to building foundations. The categorization system created by the U.S. Army Waterways Experiment Station (Snethen, 1979) is one of the most often used in the U.S., among several classification schemes [25]. Table 2 describes the classification of soil expansion according to index properties.

Table 2. Classification of Expansive Based on Index Tests [25]

LL	PI	Potential Swell (%)	Potential Swell Classification
<50	<25	< 0.5	Low
50-60	25-35	0.5-1.5	Marginal
> 60	>35	> 1.5	High

The plasticity index has also been proven to be the only test that can be utilized as a preliminary indicator for swelling behavior in the majority of clays. Tables 3 and 4 showed how clays' plasticity indices affected their swelling potential.

Table 3. Relationships between the PI and swelling potential [26]

PI	Potential Swell (%)
0-15	Low
10-35	Marginal
20-55	High
35 and above	Very high

Table 3. Expansive soil classification system based on the PI

Degree of Expansion	IS 1498 [27]	Chen [28]	Holtz & Gibbs [29]
Low	<12	<15	<20
Marginal	12-23	10-35	12-34
High	23-32	20-55	23-45
Very high	>32	>35	>32

3.4.2. Soil Samples Data Descriptions

To ascertain the distributional characteristics of each dataset and geological layer, statistical analyses were conducted, and the results were visually represented through graphical means. Tables 5 to 7 encapsulate the statistical outcomes, specifically focusing on the relationships between observed and modeled index property values for Liquid Limit (LL), Plastic Limit (PL), and Plasticity Index (PI) across the investigated soil classifications. Furthermore, these tables document the acceptable prediction errors observed between the measured and predicted values. Statistically, the models exhibit a high degree of accuracy, as evidenced by a maximum Root Mean Square Error (RMSE) of ≤ 10 and a minimum Root Mean Square Standard Deviation (RMSSD) of ≥ 0.89. These metrics, in conjunction with other statistical indicators, substantiate the reliability and precision of the results derived from the Employed Boosted Machine (EBM) methodology.

Table 4. Details of prediction errors and Statistical parameters of liquid limit samples

		Prediction errors					Statistical parameters			
Soil Layers	***Sample***	***Mean***	***RMSE***	***MSD***	***RMSSD***	***ASE***	***Range***	***Mean***	***Std. deviation***	***COV%***
Layer 1	212	0.00995	5.42	0.0034	0.964	5.398	23-59	43.116	7.397	17
Layer 2	99	-0.0047	7.278	-0.0054	0.956	7.727	28-59	43.992	9.522	22
Layer 3	129	-0.139	7.680	-0.014	0.951	8.004	25-63	43.834	8.940	20
Layer 4	107	0.096	8.316	0.015	0.998	8.245	25-61	45.353	9.192	20
Layer 5	109	0.116	8.031	0.011	0.968	8.33	27-65	47.223	9.000	19
Layer 6	69	0.088	8.066	0.0036	0.970	8.219	24-61	44.202	8.961	20
Layer 7	41	-0.120	8.672	-0.020	0.973	8.61	19-62	43.795	8.713	18
Layer 8	38	0.540	10.36	0.050	1.118	9.701	20-63	46.474	11.457	25
Layer 9	19	-0.682	5.76	-0.048	0.894	5.99	32-61	42.605	9.469	22
Layer 10	32	-0.0086	10.030	0.0105	0.960	11.086	26-69	48.039	11.991	25

Table 5. Details prediction errors and Statistical parameters of plastic limit samples

		Prediction errors					Statistical parameters			
Soil Layers	***Sample***	***Mean***	***RMSE***	***MSD***	***RMSSD***	***ASE***	***Range***	***Mean***	***Std. deviation***	***COV%***
Layer 1	212	-0.027	3.804	-0.0098	0.993	3.775	12-36	22.229	4	18
Layer 2	99	-0.056	4.65	-0.0106	0.989	4.789	9-33	21.856	4.789	22
Layer 3	129	0.0749	5.777	0.0119	0.988	5.844	9.3-45	22.111	5.769	26
Layer 4	107	0.262	5.242	0.041	0.993	5.541	9-44	22.965	3.368	23
Layer 5	109	-0.0097	2.839	-0.0043	0.970	2.922	14-29	21.882	2.850	13
Layer 6	69	0.207	5.327	0.036	0.994	5.390	3-38	21.849	5.326	24
Layer 7	41	-0.1433	9.147	-0.0139	0.97	9.396	2.7-41	22.745	9.175	40
Layer 8	38	0.128	5.149	-0.0093	0.937	5.4716	4-32	20.958	5.807	27
Layer 9	19	0.072	2.33	0.035	0.938	2.540	19-30.3	24.842	2.921	12
Layer 10	32	-0.0806	3.952	-0.0062	0.972	4.201	9-30	19.499	4.863	25

Table 6. Details prediction errors and Statistical parameters of plasticity limit samples

		Prediction errors					Statistical parameters			
Soil Layers	***Sample***	***Mean***	***RMSE***	***MSD***	***RMSSD***	***ASR***	***Range***	***Mean***	***Std. deviation***	***COV%***
Layer 1	212	0.0406	5.175	0.0053	1.0431	4.851	1.2-37	20.985	7.237	34
Layer 2	99	0.167	6.299	0.0103	0.976	6.497	1.9-37	22.136	8.801	37
Layer 3	129	-0.265	7.692	-0.0177	0.908	8.187	4.6-42	21.899	8.868	40
Layer 4	107	-0.273	8.681	-0.0290	0.999	8.699	3-40.8	22.731	9.582	42
Layer 5	109	0.0016	8.379	0.0001	0.983	8.594	8.2-42	25.341	9.291	37
Layer 6	69	0.193	9.486	0.0193	0.953	10.024	4-42.78	22.352	10.348	46
Layer 7	41	-0.035	10.142	-0.0019	0.989	10.432	4-42	21.05	10.308	49
Layer 8	38	0.163	8.872	0.033	1.053	8.063	4-41	25.515	11.172	44
Layer 9	19	-0.625	6.433	-0.0454	0.933	6.420	5.9-40	17.763	10.727	60
Layer 10	32	0.270	7.750	0.0276	0.966	9.069	9.5-42	28.541	11.210	39

Note: RMSE=Root Mean Square Error, MSD= Mean Standardized, RMSSD= Root Mean Square Standardized, ASE= Average Standard Error.

3.4.3. Model for Regression Empirical Bayesian Kriging (EBK)

EBK is a contemporary mapping technique that takes into consideration the uncertainty of parameter estimates in functions reflecting the changes in property variance with the expansion of the survey region (variograms). According to operation manuals, EBK is a technique for geostatistical interpolation that automates the most challenging parts of creating a good kriging model [20]. In contrast to conventional kriging techniques, EBK enables taking into account the uncertainty associated with the charting of variograms [30]. However, because the variogram's uncertainty is not taken into consideration, it is implicitly assumed that the variogram computed from experimental points represents the genuine variogram over the surveyed area. It is essential to mention that.

The current version of the summary EBK algorithm is a heuristic algorithm. There are undoubtedly circumstances in which such algorithms can have a formal mathematical and statistical justification, but their theoretical foundations are now wholly lacking. The prerequisites for the method's instructions also have a number of gaps. In addition to generating prediction surfaces, the EBK algorithm produces a prediction standard error (PSE) surface for each property, representing the uncertainty associated with the estimated values. These PSE maps serve as spatially explicit confidence intervals, allowing visual assessment of prediction reliability. Areas with denser sampling typically show lower PSE values, whereas zones with sparse borehole distribution exhibit higher uncertainty.

This can be utilized to identify index properties. By sequentially excluding experimental points from the population and calculating their interpolated value, cross-validation was used to gauge the quality of the resulting cartograms. The mean interpolation error (ME).

$$ME = \frac{\sum_{i=1}^{n} \check{Z}(x_i) - z(x_i)}{n} \quad (1)$$

and the interpolation mean squared error (RMSR)

$$RMSR = \sqrt{\frac{\sum_{i=1}^{n} \check{Z}(x_i) - z(x_i)}{n}} \quad (2)$$

where $\check{Z}(x_i)$ is the value following interpolation, $z(x_i)$ represents the measured value at the point x_i, n is the number of data.

3.4.4. Spatial Interpolation

A variogram can be used to describe the spatial variability of a characteristic. The function demonstrates how the property variance evolves as the distance between sampling locations increases [31]. Microsoft Excel 2010 was used to execute statistical computations; Geostatistical Analyst for ArcGIS 10.7.2 was used to plot and analyze cartograms. Data were displayed as normalized deviations (z) to show the geographic variability's structure.

$$z = \frac{x - \mu}{\sigma} \quad (3)$$

where, x represents the index property value, μ is the mean value, σ represents the standard deviation.

3.4.5. Theoretical Approach

The theoretical basis of the research is premised on the principles of geostatistics, specifically spatial autocorrelation, which presupposes the existence of a greater likelihood of similarity of geotechnical properties between spatially proximate rather than distant soil samples. The conceptual framework of Kriging and other spatial interpolation techniques is based on this principle, which is also known as the First Law of Geography as introduced by Tobler. Classical kriging, like ordinary or Universal Kriging, uses a motionless random field, or in other words, the mean and the variance of a variable remain the same everywhere. Nevertheless, there are hardly ever natural soils that are not mobile; their characteristics are in a constant state of flux as a result of the complicated processes of deposition, climate, and geomorphological processes. Empirical Bayesian Kriging (EBK) in this sense offers a solid theoretical improvement.

EBK uses Bayesian inference in the kriging model, but instead of taking variogram parameters (e.g., nugget, sill, and range) as deterministic, they are random variables that are assigned prior distributions. Through conditional simulations, these parameters are successively updated, resulting in a posterior distribution more representative of uncertainty. Contrary to classical Kriging, which generates a single deterministic estimate, EBK takes due cognizance of the stochasticity of spatial variability and gives probabilistic confidence intervals of every prediction. In the current study, the theoretical approach allows a more realistic description of the spatial variability of Liquid Limit (LL), Plastic Limit (PL), and Plasticity Index (PI) over Thi Qar province. The EBK framework therefore fills the gap between theoretical geostatistics and practical geotechnical mapping and has been shown to guarantee that predictions include the uncertainty of measurement, as well as the spatial heterogeneity.

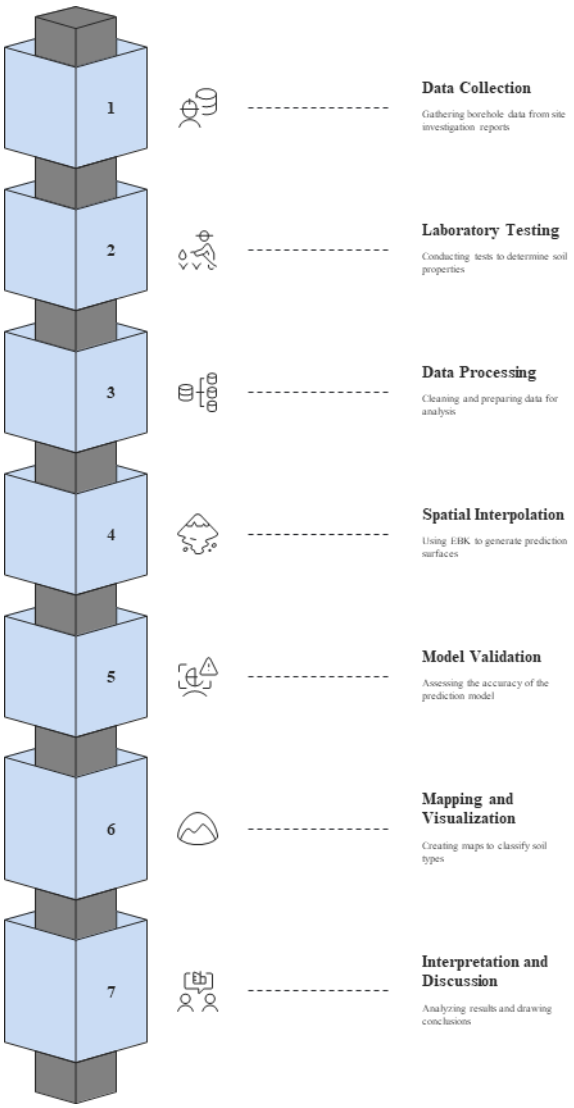

Figure 3. The Methodology Flowchart

4. Results

The liquid limit, plastic limit, and plasticity index values were imported into ArcGIS up to a depth of 20 m. The chosen values are rounded to the area to calculate the soil attributes' geographical distribution. The distribution of each depth data set was determined using statistical features in ArcGIS, and graphs were generated to determine the soil typology of each layer. The data were extrapolated over the chosen area to determine how the liquid limit was distributed spatially. Statistical figures and images were created to determine the data distribution for each depth.

4.1. Liquid Limit (LL)

The spatial distribution of Liquid Limit (LL) across ten 2-meter depth intervals (0-20 m) in the Thi Qar Region, Iraq, was mapped to characterize soil properties. LL values ranged from 32% to 69% across all depths. Generally, higher LL zones, indicative of silt- and clay-rich soils, were prevalent in the northern and central parts of the study area.

Specifically, the (0-2) m layer (Figure 4-a) was predominantly characterized by LL values of 43.4-50% (blue and dark blue), suggesting a significant content (>50%) of silt and clay. Lower LL values (32-39%, indicating alluvial sand) were observed in the eastern region.

In the (2-4) m layer (Figure 4-b), the spatial extent of alluvial sand (LL 26-32%, green and dark green) increased, covering approximately 50% of the area, with the remaining portion (blue and dark blue) exhibiting higher LL values.

At the (4-6) m depth (Figure 4-c), the majority of the map displayed blue hues (LL 44.7-52.2%), indicating a return to silt and clay-rich soils (>50% content), similar to the uppermost layer.

For the (6-8) m layer (Figure 4-d), approximately 75% of the area showed LL values between 43.3-49.7%, with higher values (49.7-54.8%) concentrated in the far south and scattered central locations. Few areas exhibited lower LL values (35.3-43.3%, green).

At the (8-10) m depth (Figure 4-e), LL values decreased in the far south (37.3-43.9%, green) and increased in the north (48-54.7%).

The (10-12) m layer (Figure 4-f) showed an overall increase in the LL range with depth, with the lowest values (36-41.5%, green) appearing in scattered, limited areas.

Layers 7 (12-14 m), 9 (16-18 m), and 10 (18-20 m) (Figure 4-g, 4-i, and 4-j, respectively) generally exhibited the highest LL values across the study area, ranging from 32% to 63%. An exception was observed in layer 8 (14-16 m) in the eastern part, where LL values ranged from 20% to 32% (Figure 4-h).

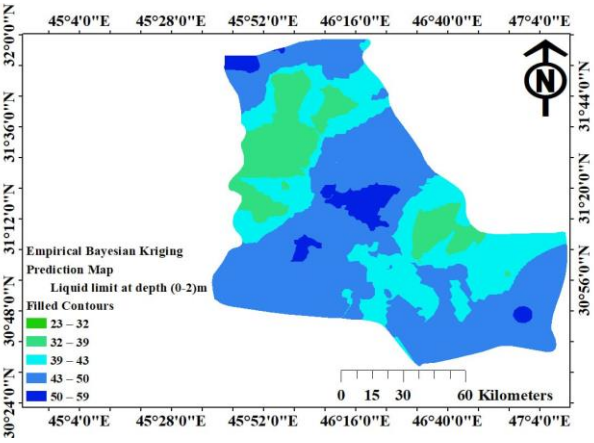

(a) LL at a depth of (0-2) m

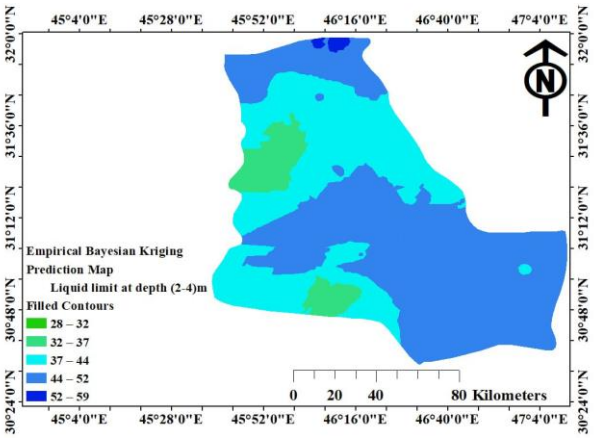

(b) LL at a depth of (2-4) m

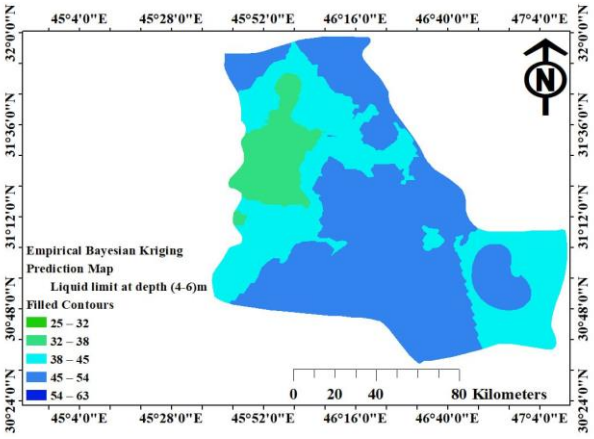

(c) LL at a depth of (4-6) m

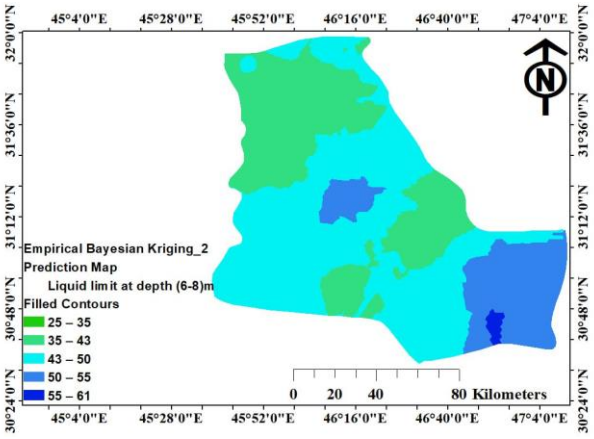

(d) LL at a depth of (6-8) m

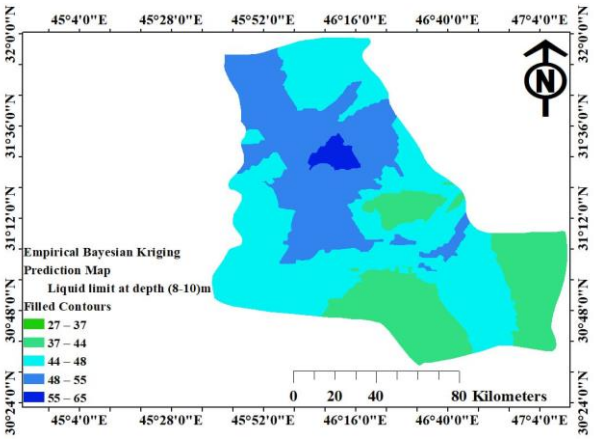

(e) LL at a depth of (8-10) m

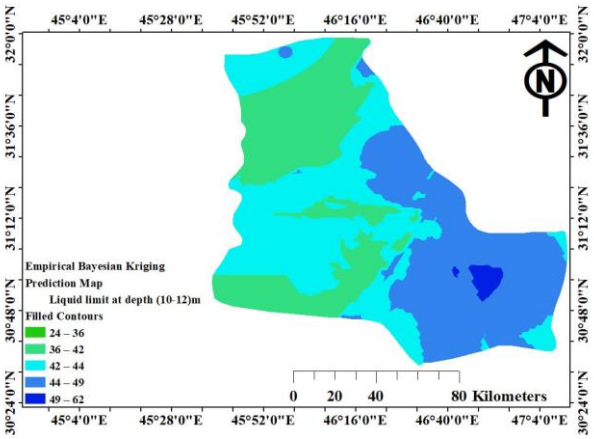

(f) LL at a depth of (10-12) m

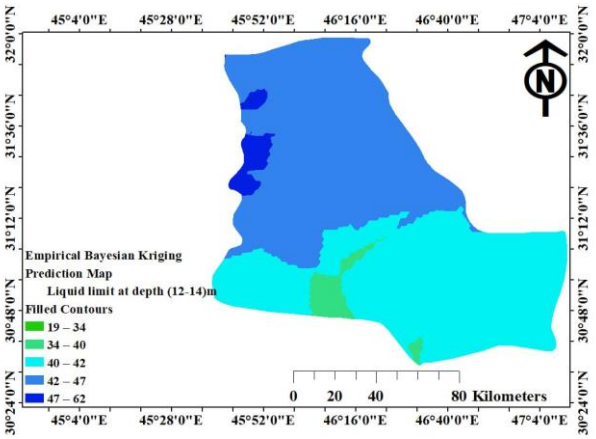

(g) LL at a depth of (12-14) m

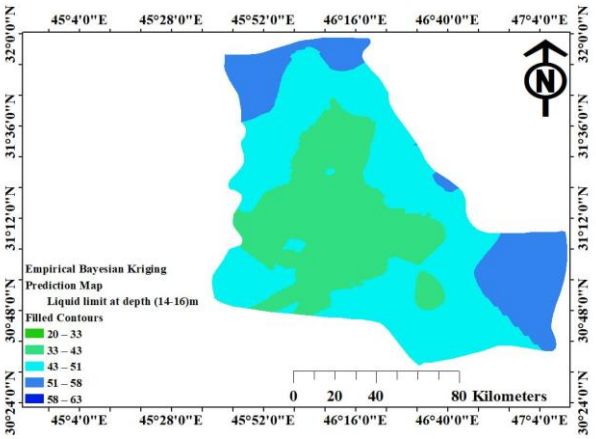

(i) LL at a depth of (14-16) m

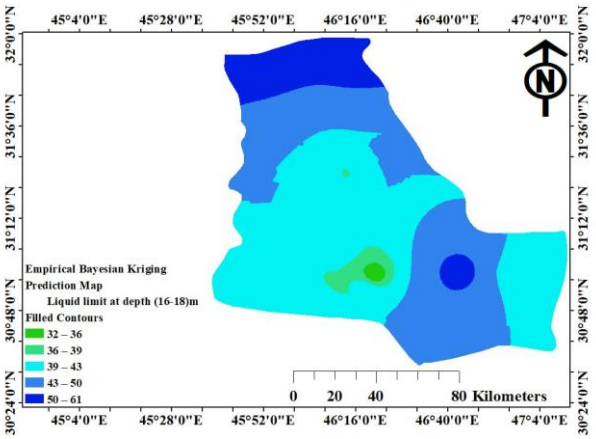

(j) LL at a depth of (16-18) m

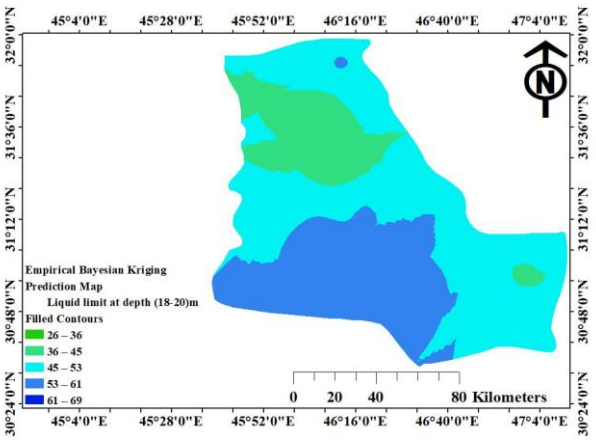

(j) LL at a depth of (18-20) m

Figure 4. Spatial Distribution map of the LL in the soil of Thi Qar

The Root Mean Square Standardized Error (RMSSD) values for the predicted versus measured LL for each 2-meter interval were (0.960, 0.894, 1.118, 0.973, 0.970, 0.968, 0.998, 0.951, 0.956, 0.964). These RMSSD values, derived from the Empirical Bayesian Kriging (EBK) method, confirm a strong and highly satisfactory correlation between the measured and predicted LL values across all depth intervals.

4.2. Plastic Limit (PL)

At the transition between the plastic and semi-solid stages, a soil plastic limit is expressed in terms of its water content, expressed as a percentage. A soil that demonstrates flexibility over a range of water contents and retains its shape after drying is referred to as plastic soil (ASTM D4318) [23].

The resulting maps of the PI characteristic according to the EBK method are shown in Figures 5-a, 5-b, 5-c, 5-d, 5-e, 5-f, 5-g, 5-i, 5-j, and 5-k, respectively. The maps display the vertical soil layers at various depths, with a thickness of 2 m for each layer. The lowest values of the PL appear in dark green, and the values range (from 9 to 21%) and represent very few areas in all layers of the soil, except the northern region defined by Al-Rifai and parts of Al-Shatrah for layer 4, which means the depth (6-8 m). The light greens occupy this layer's central and southern regions, in which the PL value ranges around 21-26%. The highest value of PL is displayed on the maps in dark blue, and it is almost non-existent in most maps; if present, it appears within Layer 9 and Layer 10 in the south. The value of PL, which occupies the largest area in all the maps of the soil layers, is in the range of 19-26% and shows the gradation of light green and light blue.

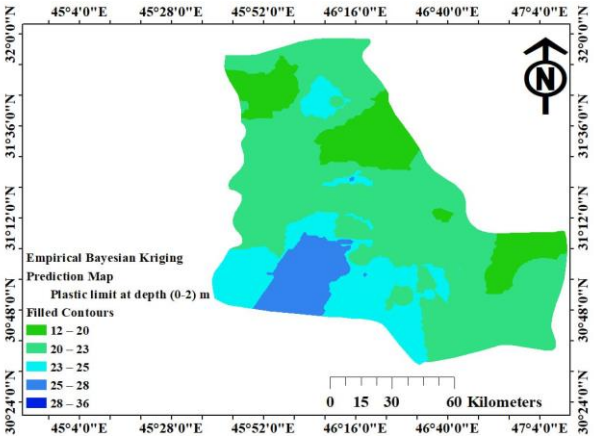

(a) PL at (0-2) m.

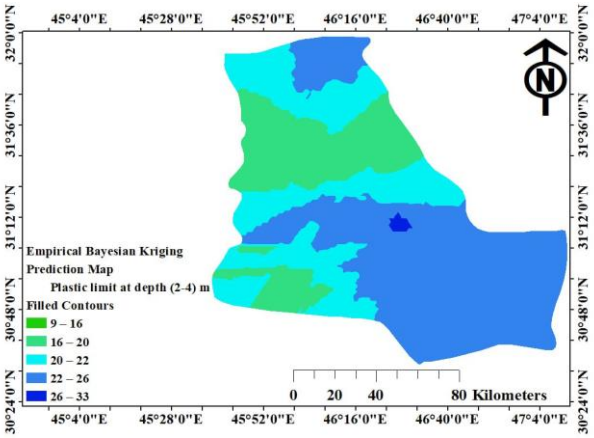

(b) PL at (2-4) m.

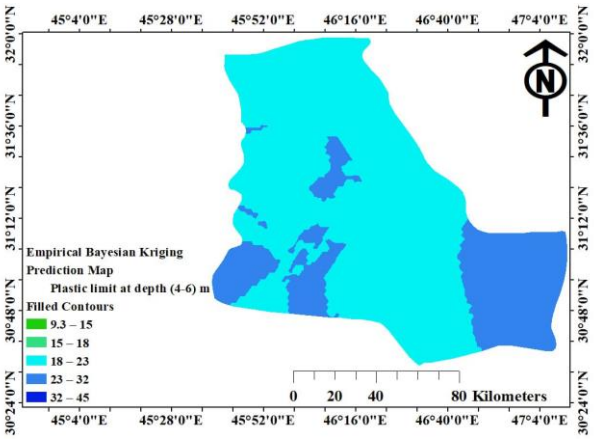

(c) PL at (4-6) m.

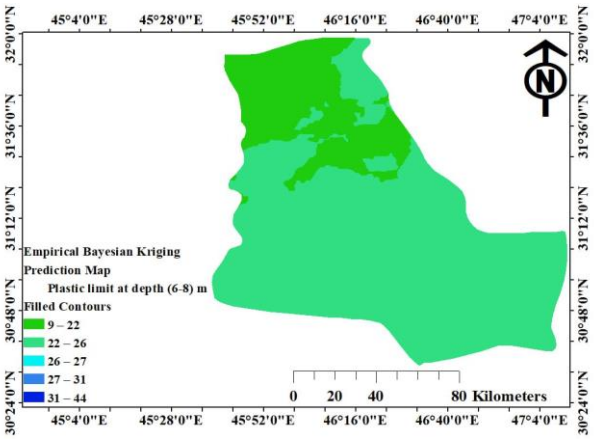

(d) PL at (6-8) m.

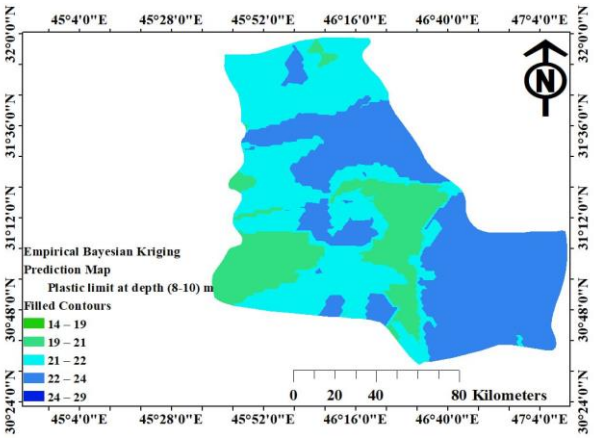

(e) PL at (8-10) m.

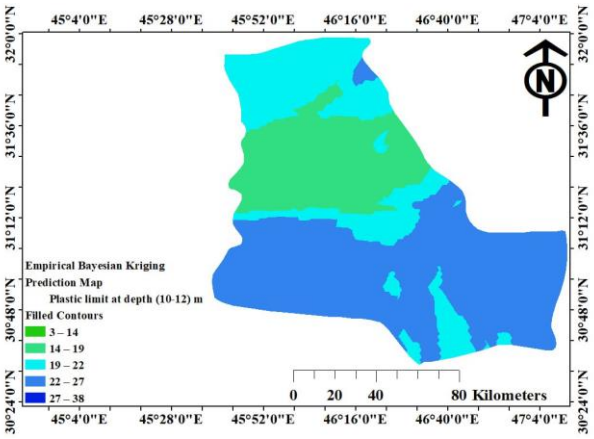

(f) PL at (10-12) m.

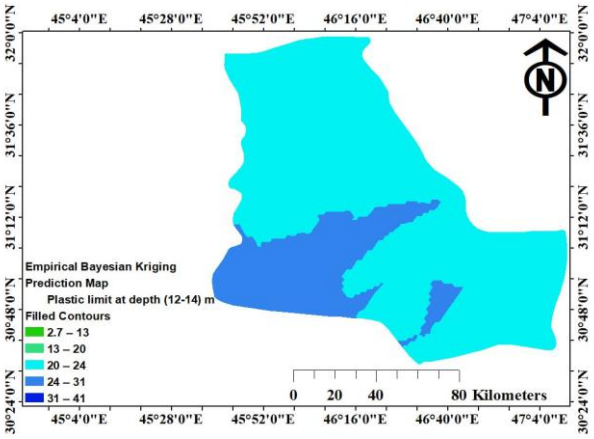

(g) PL at a (12-14) m.

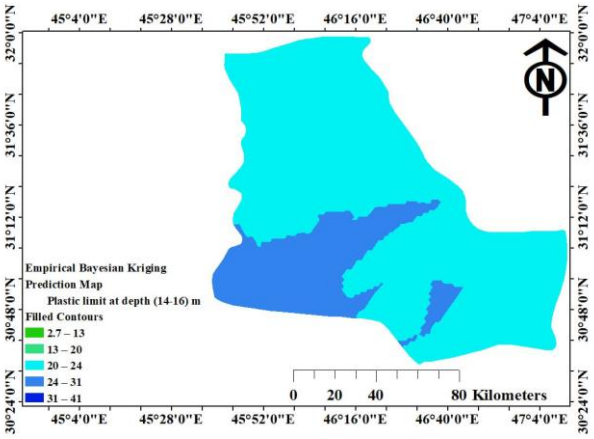

(i) PL at (14-16) m.

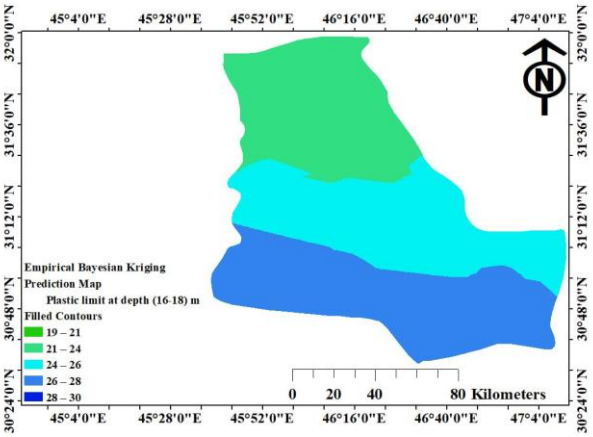

(j) PL at (16-18) m.

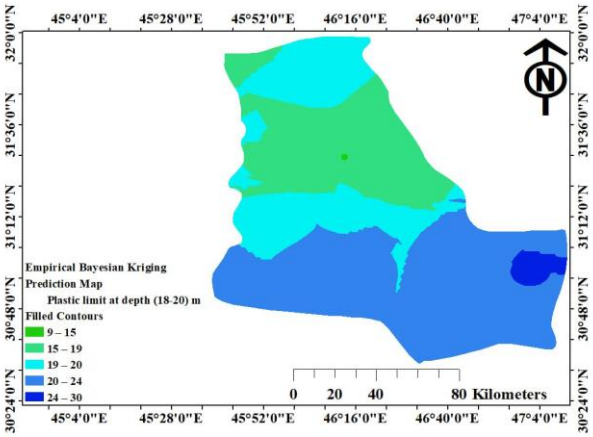

(k) PL at (18-20) m.

Figure 5. Spatial Distribution of the Plastic Limit (PL) at Ten Layers

The results show that the RMSSD values for the anticipated versus measured plastic limit are 0.972, 0.938, 0.937, 0.97, 0.994, 0.970, 0.993, 0.988, 0.989, and 0.993 for layer 1, layer 2, layer 3, layer 4, layer 5, layer 6, layer 7, layer 8, layer 9, and layer 10, respectively. From the statistical perspective, the results show values with a strong correlation and the lowest possible error rate.

The spatial variation of PL suggests localized zones of coarse-grained soil in the eastern areas, likely associated with more recent alluvial deposits from the Euphrates River. The relatively low PL values (9% to 21%) in these regions indicate a lower clay content and limited plastic deformation capacity. This pattern aligns with the grain-size analysis, which confirms a dominance of silty sand and sandy silt textures in those areas.

4.3. Plasticity Index (PI)

The range of water content over which soil exhibits plastic behavior is known as the plasticity index (PI). It is expressed mathematically as the distinction between the liquid and plastic limits:

$$PI=LL-PL \quad (4)$$

The predicted spatial distribution of PI across Thi Qar province at various depths is illustrated in maps (Figures 6a to 6k). The Root Mean Square Standardized Error (RMSSD) values for the predicted versus measured PI for each layer were (0.966, 0.933, 1.053, 0.989, 0.953, 0.983, 0.999, 0.908, 0.976, 1.0431, 0.993), indicating a strong correlation between the measured and predicted PI values.

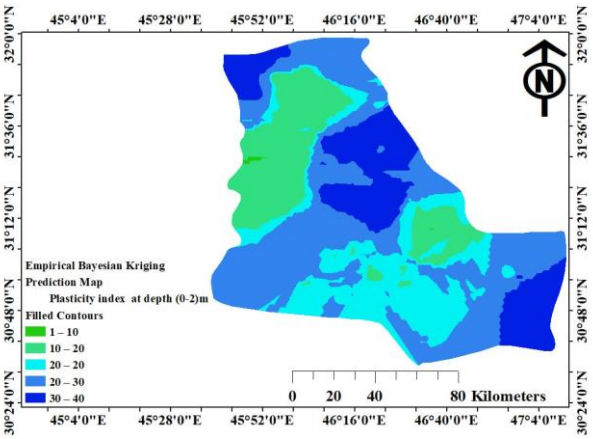

(a) PI at (0-2) m.

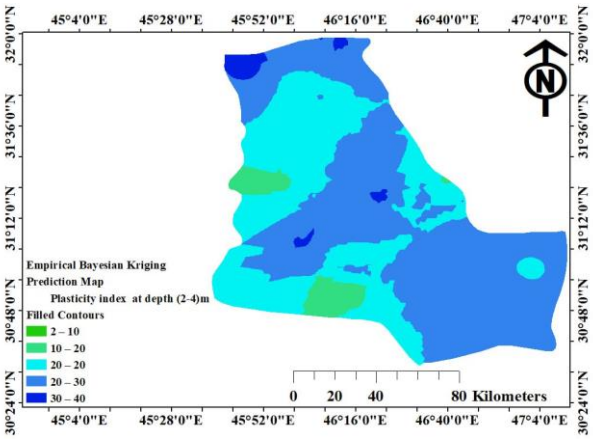

(b) PI at (2-4) m.

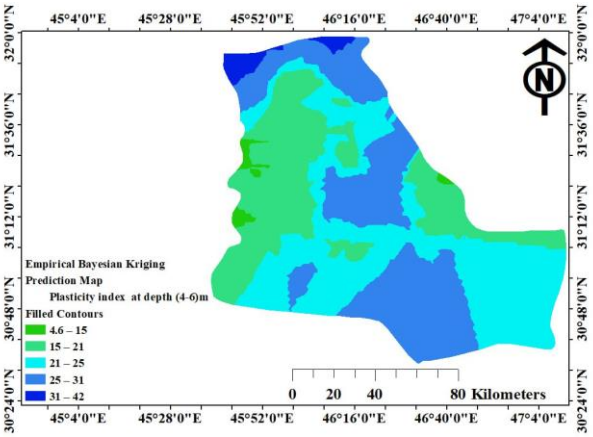

(c) PI at (4-6) m.

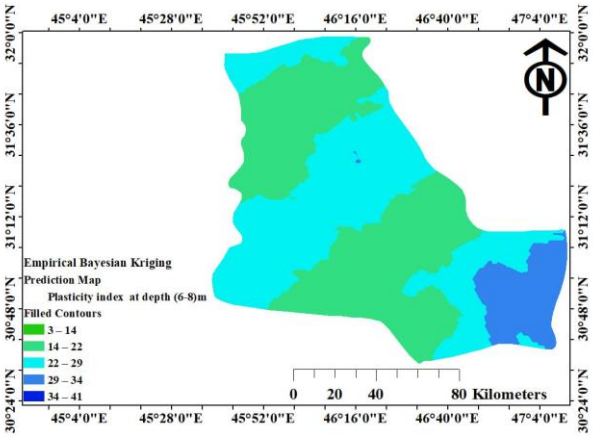

(d) PI at (6-8) m.

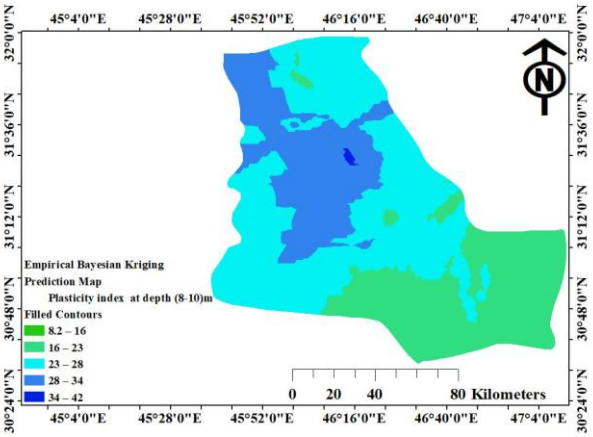

(e) PI at (8-10) m.

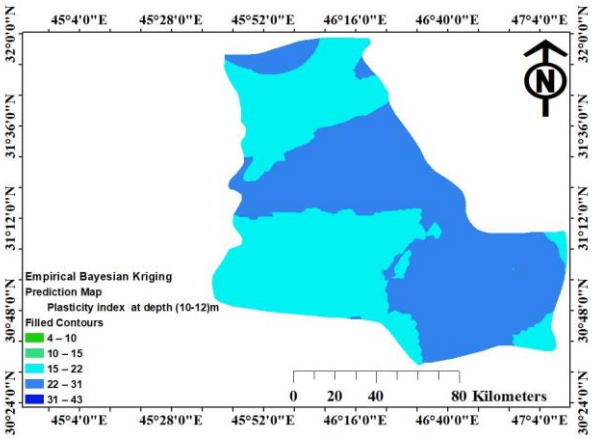

(f) PI at (10-12) m

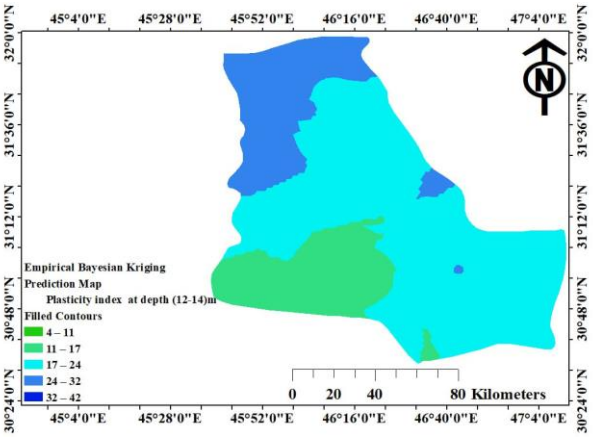

(g) PI at (12-14) m.

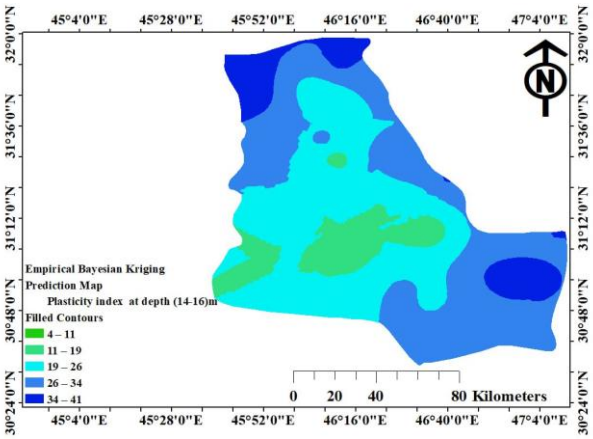

(h) PI at (14-16) m.

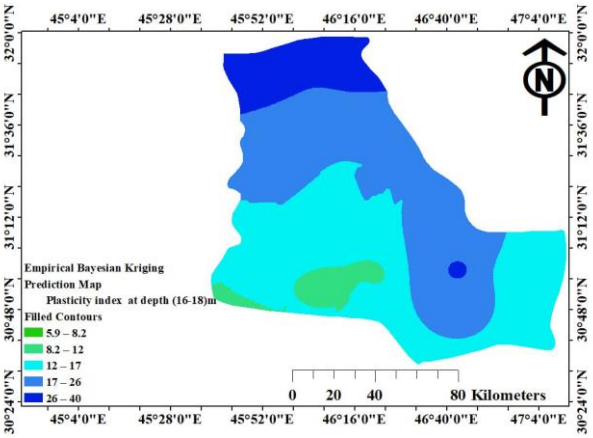

(i) PI at (16-18) m

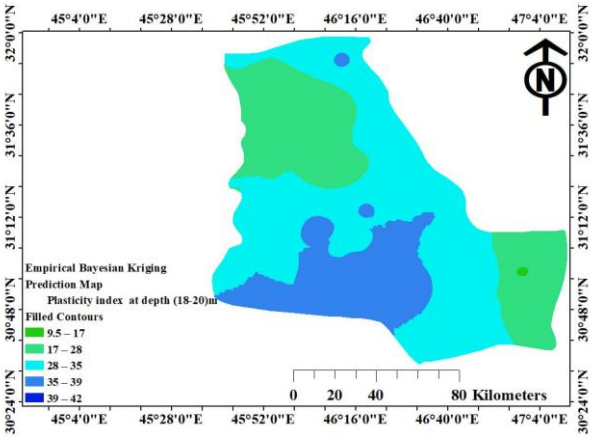

(j) PI at (18-20) m.

Figure 6. Spatial Distribution of the Plasticity Index for Ten Layers

The PI values across the soil profile ranged approximately from 1% to 39%, with the majority of the area, both horizontally and vertically, exhibiting PI values between 10% and 35%. These PI values suggest the swelling potential of the studied soil. Based on the observed PI ranges, all soil layers in the Thi Qar region are classified as having low to medium (marginal) swelling characteristics. This reflects the influence of the PI on the extent of soil swelling.

The PI maps indicate that Thi Qar soils have a majority of medium- to low-plasticity range (10-35%), which means that they have low swelling potential. The overlapping of the spatial distribution of high PI and high LL value areas establishes that there is interdependence between the clay mineral content and soil plasticity. These results are at par with Chen (2012) [12] and Holtz & Gibbs (1956) [29], who attributed high PI value to soils that contain a lot of smectite in arid areas.

According to the standard classification systems (see Tables 2 to 4), the soils of the Thi Qar region are defined as having low to medium (marginal) swelling potential. This implies that expansive soils exist, but in most cases, their swelling nature can be controlled as per the geotechnical engineering understanding. The EBK model proved to be highly predictive of PI, whose RMSSD of all the layers ranged between 0.908 and 1.053, giving a high level of confidence in the maps generated (Table 8).

Table 7. Summary of Spatial Prediction Results and Validation Metrics for Soil Index Properties

Layer	Depth (m)	Property	Value Range (%)	Predominant Range (%)	RMSSD
1	0-2	LL	32 - 59	43 - 50	0.964
		PL	12 - 36	19 - 26	0.993
		PI	1 - 37	10 - 35	1.043
2	2-4	LL	26 - 59	26 - 32 & 44 - 51	0.956
		PL	9 - 33	19 - 26	0.989
		PI	2 - 37	10 - 35	0.976
3	4-6	LL	25 - 63	45 - 52	0.951
		PL	9 - 45	19 - 26	0.988
		PI	5 - 42	10 - 35	0.908
4	6-8	LL	25 - 61	43 - 50	0.998
		PL	9 - 44	21 - 26	0.993
		PI	3 - 41	10 - 35	0.999
5	8-10	LL	27 - 65	44 - 55	0.968
		PL	14 - 29	19 - 26	0.970
		PI	8 - 42	10 - 35	0.983
6	10-12	LL	24 - 61	42 - 53	0.970
		PL	3 - 38	19 - 26	0.994
		PI	4 - 43	10 - 35	0.953
7	12-14	LL	19 - 62	44 - 55	0.973
		PL	3 - 41	19 - 26	0.970
		PI	4 - 42	10 - 35	0.989
8	14-16	LL	20 - 63	43 - 55	1.118
		PL	4 - 32	19 - 26	0.937
		PI	4 - 41	10 - 35	1.053
9	16-18	LL	32 - 61	42 - 53	0.894
		PL	19 - 30	19 - 26	0.938
		PI	6 - 40	10 - 35	0.933
10	18-20	LL	26 - 69	48 - 59	0.960
		PL	9 - 30	19 - 26	0.972
		PI	9 - 42	10 - 35	0.966

4.4. General Soil Composition

The most commonly found soil components in the Thi Qar study area include silt, clay, and minor levels of sand. These are the types of soils that have unique geotechnical characteristics, and they are all of significance whenever undertaking a civil engineering project. Thus, proper soil investigation before starting the projects is important to ascertain the type and behavior of soil. The suitability of certain geotechnical tests is also intrinsically connected with the composition of soil. In the GIS setting, statistical results are converted to positional maps, which allow a spatially explicit interpretation of the soil distribution.

EBK-based prediction standard error maps show that the interpolation uncertainty in the Thi Qar province is generally low, and the PSE values represent less than 10 percent of the average property values in the province. The central and northern regions have the lowest level of uncertainty because the borehole density is the greatest, and the values of errors are somewhat higher in the southeastern region, which indicates inadequate coverage of the area. This trend supports the point that the data distribution is a powerful regulator of the model accuracy, and the EBK initiate can be successfully used to estimate this uncertainty in the ultimate spatial forecasts.

4.5. Depth-Dependent Plasticity and Soil Classification

To further describe the cohesive soils, plasticity charts (Figure 7) were created at each of the 2-meter depths, which helped in classifying the soils based on the Unified Soil Classification System (USCS). The soils were mainly characterized as inorganic clays of moderate plasticity (CL) and high plasticity (CH), which were evidence of high concentrations of clay minerals. The majority of samples were above the A-line, and it proved the nature of their cohesiveness. The correlation between Plasticity Index (PI) and Liquid Limit (LL) was measured against each layer, and a general linear trend (PI = a LL - b) was observed, with the magnitude of the correlation as the coefficient of determination (R2) differing significantly with depth (Table IX). Increased R2 values indicate increased homogeneity, and reduced R2 values indicate increased heterogeneity in individual layers, which may be due to interbedded silts and clays of different mineralogies. These variations with depth highlight the complicated history of the deposition of the Mesopotamian Plain. As illustrated in Figure 7, Layer 1 has a cluster of data points within the predominant CL and CH regions of the plasticity chart. This visual difference between Layer 7 (Figure 7) and Layer 3 (Figure 5) is the increased scatter of the data points, which is associated with the lower R^2 value in Table 9 and represents more heterogeneous soils. On comparing the plasticity charts in Figure 7, there is an overall tendency of rising LL with the depth, as it was in Layers 9 and 10. Table 9 gave the equations and the R^2 value of each layer, which gives a quantitative foundation to the variability in soil plasticity between its vertical levels.

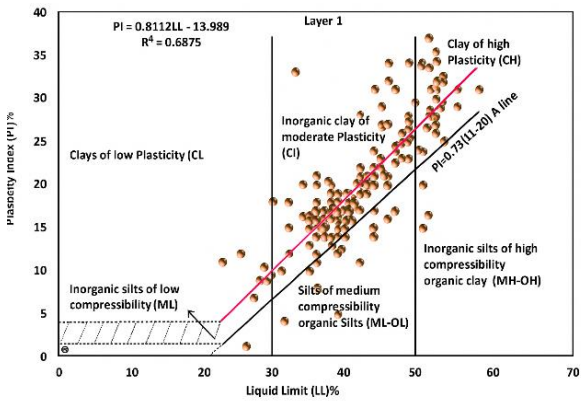

(a) At depth (0-2) m

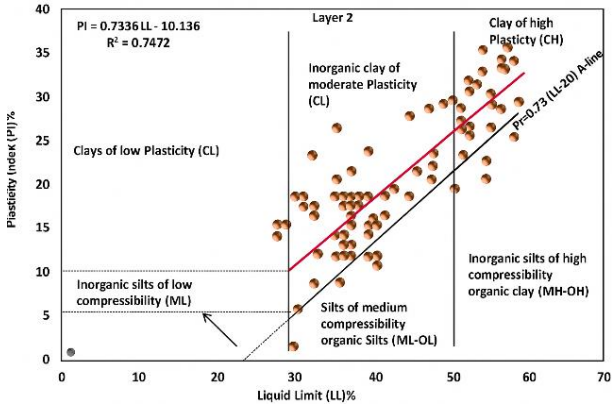

(b) At depth (2-4) m

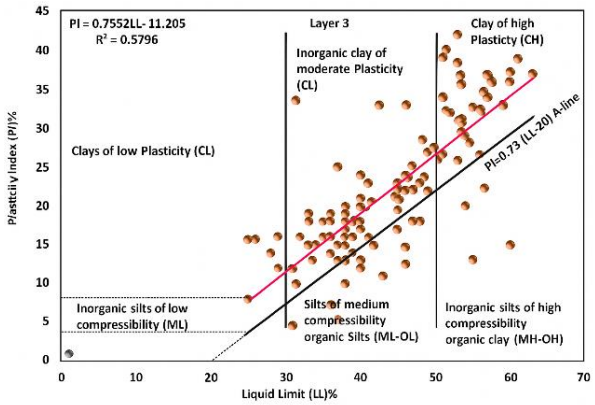

(c) At depth (4-6) m

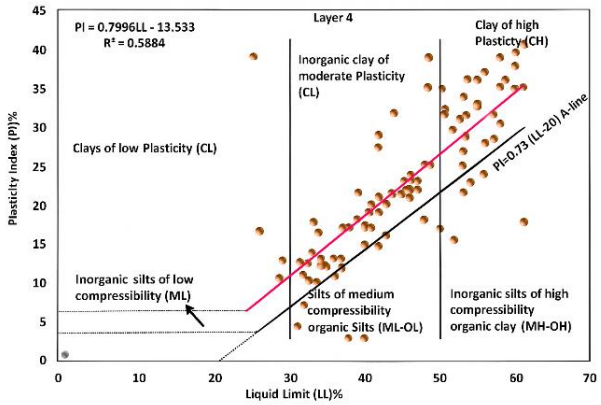

(d) At depth (6-8) m

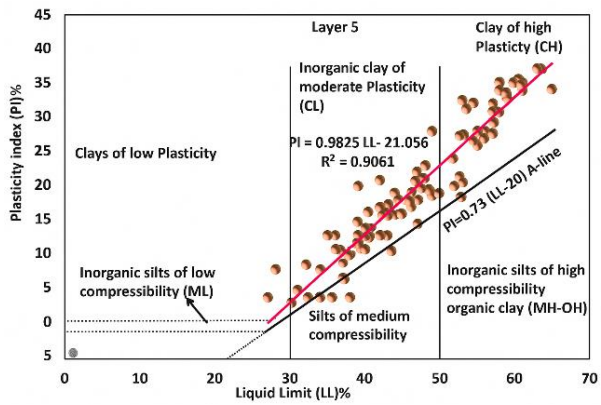

(e) At depth (8-10) m

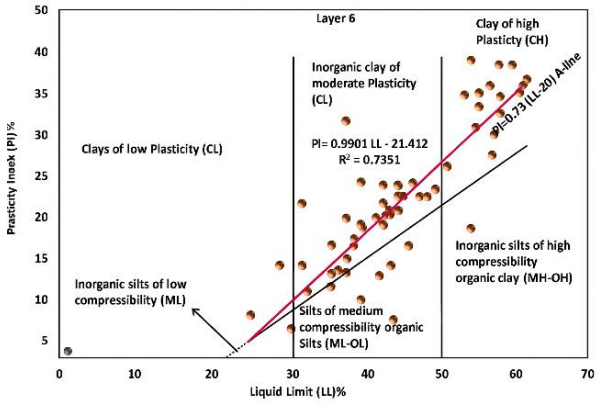

(f) At Depth (10-12) m

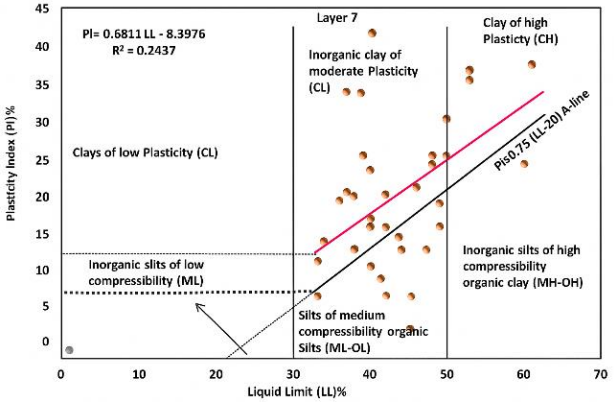

(g) At depth (12-14) m

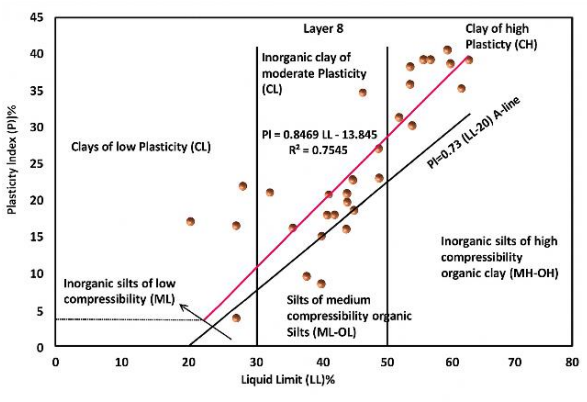

(h) At depth (14-16)

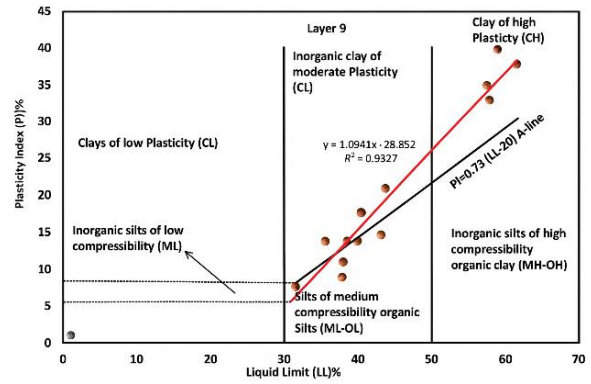

(i) At Depth (16-18) m

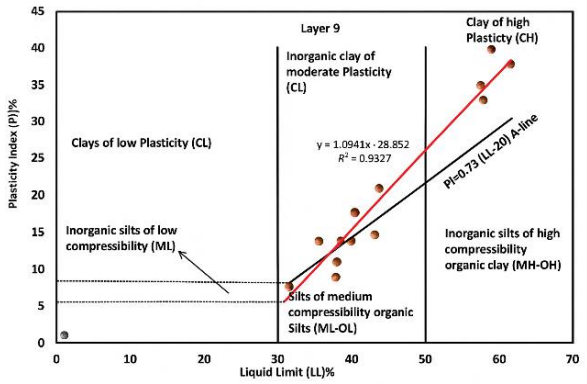

(j) At depth (18-20) m

Figure 7. Plasticity Charts of the Cohesive Soil for Ten Layers

Table 8. Summary of Plasticity Characteristics and Correlations by Soil Layer

Layer	Depth (m)	Predominant Soil Class (USCS)	PI vs. LL Correlation Equation	R^2
1	0-2	CL, CH	$PI = 0.80 * LL - 14$	0.69
2	2-4	CL, CH	$PI = 0.73 * LL - 10.00$	0.75
3	4-6	CL, CH	$PI = 0.76 * LL - 11.21$	0.58
4	6-8	CL, CH	$PI = 0.80 * LL - 13.53$	0.59
5	8-10	CL, CH	$PI = 0.76 * LL - 11.21$	0.82
6	10-12	CH, CL	$PI = 0.99 * LL - 21.41$	0.74
7	12-14	CL, ML-OL	$PI = 0.68 * LL - 8.40$	0.24
8	14-16	CH, CL	$PI = 0.85 * LL - 13.85$	0.75
9	16-18	ML-OL, CL, CH	$PI = 1.09 * LL - 28.85$	0.93
10	18-20	CH, CL	$PI = 0.85 * LL - 12.52$	0.84

5. Discussion

5.1. Geology and Geomorphology Effects on the Spatial Patterns

The conspicuous occurrence of higher Liquid Limit (LL) ranges in the northern and central regions of Thi Qar province, indicating finer-grained and highly plastic soils, can be directly linked to the region's fluvial–lacustrine depositional environment. Thi Qar lies on the Mesopotamian Plain, a vast alluvial area formed by the Euphrates and Tigris rivers. The deposition of silts and clays is commonly observed in downstream areas of major river channels, such as old floodplains, oxbow lakes, and low-energy backswamps. The vertical uniformity of soils with medium plasticity (CL) and high plasticity (CH) across different depths confirms the widespread presence of cohesive soils. The occurrence of CH soils, in particular, suggests the presence of clay minerals from the smectite group (montmorillonite), which are highly prevalent in arid and semi-arid lacustrine and fluvial deposits.

On the other hand, low LL values—especially where alluvial sand was observed in the eastern part at depths of 0.5 to 2 m—are associated with active fluvial processes. Major water bodies, such as the Euphrates River and the Al-Gharraf stream, indicate high-energy flow regimes that favor the deposition of coarser sediments (sands and silty sands) near active or former channels and their incised valleys. This results in clear spatial variability: coarser, less plastic soils occur in areas directly influenced by energetic water flow, while more plastic soils accumulate in calmer depositional environments.

Certain anomalies, including significantly reduced Plastic Limit (PL) values observed in the northern part of Al-Rifai and parts of Al-Shatrah at depths of 6–8 m, require further geological investigation. These local variations, where PL values range between 9% and 21%, indicate less plastic soil structures compared to surrounding areas. This may suggest the presence of paleochannels, ancient river terraces, or localized geological features where coarser sediments (such as sands or silts) were deposited during specific geological periods or where different source materials were introduced. Such variability highlights the importance of detailed, layer-by-layer mapping to capture the three-dimensional heterogeneity of the soil profile, which is essential for accurate geotechnical assessment.

5.2. Influence of Arid Climate

The arid desert climate of Thi Qar, characterized by extreme temperatures and low annual rainfall (100–180 mm), exerts a direct influence on the geotechnical behavior of its clayey soils. Repeated wetting–drying cycles common in such semi-arid regions promote desiccation cracking, which weakens the soil's near-surface structure and increases permeability and anisotropy. Prolonged exposure to high temperatures and evaporation favors mineral alteration, where smectite may transform to illite or kaolinite, reducing plasticity in some layers while inducing irreversible shrinkage on rewetting. These climatic effects, coupled with the dominance of fine-grained lacustrine deposits, contribute to the cyclic swelling and shrinkage behavior observed in the province. The moderate Plasticity Index (10–35%) across most of the area reflects this balance—sufficient clay content to permit volumetric change, yet limited by mineral desiccation and partial cementation processes. Consequently, Thi Qar's climate not only shapes the physical weathering regime but also governs the long-term stability and deformation potential of its expansive soils, with direct implications for foundation design and the maintenance of surface infrastructure.

5.3. Depth-Related Trends

The depth-related analysis of soil properties provides insight into the depositional history and subsequent diagenetic processes. From a temporal perspective, it can be observed that Layers 7 (12–14 m), 9 (16–18 m), and 10 (18–20 m) exhibit relatively high liquid limit (LL) values across the study area, indicating a systematic change in soil characteristics with increasing depth.

Higher LL values at greater depths are typically associated with older, more consolidated geological strata or distinct depositional periods. This observation suggests the influence of several possible processes. First, different depositional environments may be represented at depth; older lacustrine deposits or relic marine sediments—formed when the Arabian Gulf extended further inland—are often finer-grained and more plastic in nature. Second, diagenetic processes may have altered the buried clays over geological time, as physical and chemical changes can modify mineralogy and soil fabric, thereby affecting plasticity characteristics. Third, reduced weathering at greater depths plays a role, since subsurface soils are not exposed to surface processes such as leaching, oxidation, or organic matter degradation, which may otherwise decrease soil plasticity.

Moreover, the variability in the coefficient of determination (R^2) for the linear relationship between the plasticity index (PI) and liquid limit (LL) across different layers (ranging from 0.2436 in Layer 7 to 0.93 in Layer 8) indicates significant differences in soil homogeneity and composition with depth. A high R^2 value (e.g., 0.93 in Layer 8) reflects a strong and predictable linear relationship, suggesting relatively homogeneous soil composition or the dominance of a specific clay mineralogy within that layer. In such cases, changes in clay content or type lead to a predictable response in PI. In contrast, a low R^2 value (e.g., 0.2436 in Layer 7) indicates greater heterogeneity, which may result from a complex mixture of soil textures (such as interbedded silts, sands, and clays of varying plasticity) or a more diverse clay mineral composition, leading to less predictable behavior between LL and PI.

The movement of sediment loads across the Mesopotamian Plain over geological time has produced a complex, stratified sediment profile that requires thorough geotechnical characterization. This stratification reflects long-term alluvial and lacustrine processes that have created heterogeneous layers, which in turn influence engineering performance.

The results of this study for Thi Qar Province are consistent with the available geotechnical literature, both regionally and from a methodological perspective. The observed ranges of Liquid Limit (LL), Plastic Limit (PL), and Plasticity Index (PI) in Thi Qar are comparable to those reported for other areas of the Mesopotamian Plain, including Basrah [33], Babylon [34], and An-Najaf [35]. These regions share similar alluvial and lacustrine deposits dominated by moderately to highly plastic inorganic clays (primarily CL and CH) and some silts, which are characteristic of southern Iraq. Furthermore, the presence of expansive clay minerals such as smectite aligns with previous geohydrological studies. The fact that most soils in Thi Qar exhibit low to medium swelling potential (PI 10–35) is consistent with the general understanding of clay behavior in southern Iraq and suggests a manageable engineering challenge rather than an extreme one.

The use of Empirical Bayesian Kriging (EBK) is methodologically justified due to its advantages over traditional interpolation methods such as Ordinary Kriging or Inverse Distance Weighting. EBK is particularly suitable for heterogeneous and data-limited conditions, such as those in Thi Qar, because it employs automated variogram modeling, accounts for parameter uncertainty, and produces more robust predictions [36]. The Root Mean Square Standardized Error (RMSSD) values—ranging from 0.894 to 1.118 for LL, 0.937 to 0.994 for PL, and 0.908 to 1.053 for PI—indicate high predictive performance and confirm the reliability and comparability of the study results with recent geostatistical mapping studies.

Regarding swelling potential classification, the fact that most Thi Qar soils have a Plasticity Index between 10% and 35% places them within the marginal to high swelling categories according to established classification systems, including the Unified Soil Classification System (USCS), Holtz and Gibbs [29], Chen [28], and Indian Standard IS 1498. Applying multiple classification criteria enhances confidence in the assessment of swelling potential and provides geotechnical engineers with a more nuanced understanding of soil behavior.

The internal consistency and predictive performance of the EBK model were evaluated using leave-one-out cross-validation. In this approach, each data point is sequentially removed from the dataset, and its value is predicted using the remaining data; the predicted value is then compared with the observed value to compute prediction errors. Overall prediction accuracy was assessed using the Root Mean Square Error (RMSE) and the Mean Error (ME).

Cross-validation for the Liquid Limit (LL) yielded an RMSE of 7.25 and an ME of 1.12. For the Plasticity Index (PI), the RMSE was 4.82 and the ME was −0.55. The RMSE values indicate the average magnitude of prediction errors, while the ME values suggest a slight overestimation of LL and a slight underestimation of PI by the model.

5.4. Comparison with Previous Studies

The SSLL, PSL, and PI (LL ≈ 32–69%, PL ≈ 9–45%, PI ≈ 1–39%) ranges are widely similar to the reported geotechnical mappings in the Iraqi Mesopotamian Plain, where the dominating portion is fine-grained alluvial and lacustrine. Similar studies in Basrah and Babylon record moderate to high plasticity in making encyclical clays (CL-CH), with PI typical of moderately arid alluvia: in the 10-35% range. Similar trends were also observed in Najaf–Kufa, where cohesive soils dominate in a fluvial-lacustrine depositional environment. Locally, south of Iraq, GIS mapping in Sulaymaniyah indicated similar spatial heterogeneity in Atterberg indices of borehole networks, confirming that intense lateral heterogeneity is typical of the Iraqi plains.

In terms of methodology, several previous studies in Iraq and the surrounding region have used inverse distance weighting (IDW) or traditional kriging approaches. Although these methods adequately represent first-order spatial variation, they assume constant variogram parameters and stationarity, and therefore may not sufficiently capture uncertainty in heterogeneous sedimentary formations. In contrast, the Empirical Bayesian Kriging (EBK) method used in this study accounts for parameter uncertainty through iterative simulation, producing posterior predictive surfaces with quantified uncertainty limits. Its predictive performance is comparable to or better than that typically reported for IDW and ordinary kriging under similar conditions, and evidence suggests that EBK provides more realistic transitions within complex sedimentary environments (e.g., root mean square error values and standardized errors close to 1.0 across layers in analytical studies).

Substantively, the spatial agreement observed in this study—specifically the localization of high Liquid Limit (LL) and Plasticity Index (PI) values in the north-central Thi Qar region—corresponds to the presence of finer-grained facies outside active channel networks and aligns with the fluvial-lacustrine stratigraphic model described in classical Iraqi studies. Areas with lower PL and PI values on the present maps, particularly in the eastern sectors, are associated with coarser alluvial deposits near both current and historical flow paths, consistent with previous regional assessments. The steady increase in LL values with depth, especially between 12 and 20 m, further supports the interpretation of stratified paleo-floodplain deposits reported in the literature.

Overall, these comparisons (i) confirm the validity of the spatial patterns produced in this study based on established regional evidence, and (ii) highlight the methodological advantages of EBK for provincial-scale mapping of soil index properties in semi-arid environments.

The decrease in LL and PI values with depth indicates that expansive potential progressively diminishes with increasing depth. Therefore, placing foundation elements below the upper 6–8 m of highly plastic soils can significantly reduce swelling and settlement risks within the Mesopotamian Plain. Table 8 demonstrates the regional continuity of moderate- to high-plasticity clays in southern Iraq, with variations largely controlled by depositional conditions and mineralogical composition.

Table 9. Regional comparison of geotechnical index properties across selected Iraqi provinces

Province	Typical Soil Type	Liquid Limit (LL, %)	Plastic Limit (PL, %)	Plasticity Index (PI, %)	Dominant Plasticity Class (USCS)	Main Geological/Environmental Context
Thi Qar (present study)	Clayey silt, silty clay	32–69	9–45	1–39	CL–CH	Fluvio-lacustrine deposits of the Mesopotamian Plain; semi-arid climate with cyclic wetting and drying
Basrah	Silty clay, clay	35–70	10–38	15–40	CL–CH	Deltaic deposits with marine influence; shallow groundwater and saline environment
Babylon	Clayey silt, clay	30–63	12–37	10–33	CL–CH	Fluvial sediments of Euphrates basin; moderate plasticity and high moisture variability
Najaf	Silty clay	28–55	11–32	9–27	CL	Alluvial and residual soils; slightly coarser texture and lower clay content

It is important to acknowledge that the accuracy and reliability of EBK predictions are influenced by the size and spatial distribution of the input dataset. With fewer boreholes, the uncertainty associated with the predicted LL and PI values would likely increase, potentially leading to wider prediction intervals and higher standard error values in the EBK output. A sparser dataset would also limit the ability of EBK to accurately capture local variations in soil properties, potentially resulting in a smoother and less detailed representation of the spatial distribution of LL and PI. While a formal sensitivity analysis to determine the minimum number of boreholes required for reliable predictions was beyond the scope of this study, this remains an important consideration for future research.

6. Conclusions

The paper establishes the effectiveness of combining Empirical Bayesian Kriging (EBK) and Geographic Information Systems (GIS) for mapping and analyzing geotechnical index properties across Thi Qar Province in southern Iraq. The study developed high-resolution spatial models of Liquid Limit (LL), Plastic Limit (PL), and Plasticity Index (PI) for ten soil layers down to a depth of 20 m, using data from 550 boreholes and more than 860 measurements per property. The results revealed LL values ranging from 32% to 69%, PL values from 9% to 45%, and PI values from 1% to 39%. Most soils were classified as inorganic clays of medium (CL) to high (CH) plasticity, which is characteristic of the cohesive behavior of the Mesopotamian Plain. Statistical validation showed that all properties have RMSSD values close to unity, confirming the high predictive performance of the EBK model.

The identified spatial patterns are consistent with the depositional history of the region, where the central and northern areas are dominated by fine-grained sediments, while zones near active rivers consist of coarser materials. Most soils exhibit low to moderate swelling potential (PI 10%–35%), indicating generally favorable geotechnical conditions for construction, although localized expansive areas may still exist.

The research demonstrates both theoretical and practical advantages of EBK over conventional kriging techniques, including its ability to incorporate parameter uncertainty and enhance model robustness. These attributes enable better quantification of uncertainty and more accurate spatial predictions.

The resulting geotechnical maps constitute the first comprehensive digital soil database for Thi Qar Province and provide a crucial foundation for engineering design, land-use planning, and risk assessment. Moreover, the developed framework can be applied to other semi-arid regions with limited data, supporting more informed and data-driven infrastructure development across Iraq.

7. Declarations

7.1. Author Contributions

Conceptualization, W.H. and S.K.; methodology, W.H. and S.K.; software, L.A.; validation, W.H., S.K., and L.A.; formal analysis, S.K.; investigation, W.H. and S.K.; resources, L.A.; data curation, S.K.; writing—original draft preparation, S.K.; writing—review and editing, W.H. and L.A.; visualization, S.K.; supervision, W.H.; project administration, W.H.A. All authors have read and agreed to the published version of the manuscript.

7.2. Data Availability Statement

The data presented in this study are available on request from the corresponding author.

7.3. Funding

The authors received no financial support for the research, authorship, and/or publication of this article.

7.4. Conflicts of Interest

The authors declare no conflict of interest.

8. References

[1] Razmyar, A., & Eslami, A. (2017). Geotechnical Characterization of Soils in the Eastern and Western Areas of Tehran. Engineering, Technology & Applied Science Research, 7(4), 1802–1810. doi:10.48084/etasr.1200.

[2] Karakan, E. (2022). Comparative Analysis of Atterberg Limits, Liquidity Index, Flow Index and Undrained Shear Strength Behavior in Binary Clay Mixtures. Applied Sciences (Switzerland), 12(17), 8616. doi:10.3390/app12178616.

[3] Du, J. (2023). Swelling Mechanism and Swelling Behaviour of Expansive Clay and Clay Minerals. Ph.D. Thesis, RMIT University, Melbourne, Australia.

[4] Bahl, A., Bisht, D., Mohan, C., Kothapally, T., & Reddy, G. V. (2025). Role of Clay Minerals in Geotechnical Engineering: A State-of-the-Art Review with Geotechnical Data Analysis. AIP Conference Proceedings, 3157(1), 0263675. doi:10.1063/5.0263675.

[5] Pedarla, A., Chittoori, S., & Puppala, A. (2011). Influence of mineralogy and plasticity index on the stabilization effectiveness of expansive clays. Transportation Research Record, 2212, 91–99. doi:10.3141/2212-10.

[6] Bell, F. G. (1996). Lime stabilization of clay minerals and soils. Engineering Geology, 42(4), 223–237. doi:10.1016/0013-7952(96)00028-2.

[7] Almuaythir, S., Zaini, M. S. I., & Lodhi, R. H. (2025). Predicting soil compaction parameters in expansive soils using advanced machine learning models: a comparative study. Scientific Reports, 15(1), 24018. doi:10.1038/s41598-025-09279-2.

[8] Arshid, M. U., & Kamal, M. A. (2020). Regional Geotechnical Mapping Employing Kriging on Electronic Geodatabase. Applied Sciences, 10(21), 7625. doi:10.3390/app10217625.

[9] Cheriet, F., Zerguine, A., & Cheriet, A. R. (2023). Development of a Geotechnical Database using the Geographic Information System Approach: The Case of Djelfa, Algeria. Engineering, Technology and Applied Science Research, 13(2), 10239–10242. doi:10.48084/etasr.5678.

[10] Gribov, A., & Krivoruchko, K. (2020). Empirical Bayesian kriging implementation and usage. Science of the Total Environment, 722. doi:10.1016/j.scitotenv.2020.137290.

[11] De Caires, S. A., Martin, C. S., Atwell, M. A., Kaya, F., Wuddivira, G. A., & Wuddivira, M. N. (2025). Advancing soil mapping and management using geostatistics and integrated machine learning and remote sensing techniques: a synoptic review. Discover Soil, 2(1), 53. doi:10.1007/s44378-025-00082-z.

[12] Al-Mamoori, S. K., Jasem Al-Maliki, L. A., Al-Sulttani, A. H., El-Tawil, K., Hussain, H. M., & Al-Ansari, N. (2020). Horizontal and Vertical Geotechnical Variations of Soils According to USCS Classification for the City of An-Najaf, Iraq Using GIS. Geotechnical and Geological Engineering, 38(2), 1919–1938. doi:10.1007/s10706-019-01139-x.

[13] Jalhoum, M. E. M., Abdellatif, M. A., Mohamed, E. S., Kucher, D. E., & Shokr, M. (2024). Multivariate analysis and GIS approaches for modeling and mapping soil quality and land suitability in arid zones. Heliyon, 10(5), e27577. doi:10.1016/j.heliyon.2024.e27577.

[14] Ijaz, N., Ijaz, Z., Zhou, N., Ur Rehman, Z., Abbas Jaffar, S. T., Ijaz, H., & Ijaz, A. (2025). Geotechnical Data-Driven Mapping for Resilient Infrastructure: An Augmented Spatial Interpolation Framework. Buildings, 15(17), 3211. doi:10.3390/buildings15173211.

[15] Utepov, Y., Aldungarova, A., Mukhamejanova, A., Awwad, T., Karaulov, S., & Makasheva, I. (2025). Voxel Interpolation of Geotechnical Properties and Soil Classification Based on Empirical Bayesian Kriging and Best-Fit Convergence Function. Buildings, 15(14), 2452. doi:10.3390/buildings15142452.

[16] Viegas, J., Gallardo, A., Costa, A. C., & Marinaro, R. (2024). Uncovering soft soils with 3D Empirical Bayesian Kriging A case study on cone penetration test data. Geotechnical Engineering Challenges to Meet Current and Emerging Needs of Society, 917–922, CRC Press, Boca Raton, United States. doi:10.1201/9781003431749-157.

[17] Miao, C., & Wang, Y. (2024). Interpolation of non-stationary geo-data using Kriging with sparse representation of covariance function. Computers and Geotechnics, 169. doi:10.1016/j.compgeo.2024.106183.

[18] Tzampoglou, P., Loukidis, D., Tsangaratos, P., Anastasiades, A., & Karalis, K. (2025). Correlation Between Geotechnical Indexes and Landslide Occurrence in Southwestern Cyprus Using GIS and Machine Learning. Geotechnical and Geological Engineering, 43(1), 43. doi:10.1007/s10706-024-03031-9.

[19] Yıldız, Ö. (2024). Integrated GIS-Based Mapping and ANFIS Modelling for Seismic and Geotechnical Characterization of Soil Properties. KSCE Journal of Civil Engineering, 28(9), 3708–3721. doi:10.1007/s12205-024-2262-2.

[20] Zaresefat, M., Derakhshani, R., & Griffioen, J. (2024). Empirical Bayesian Kriging, a Robust Method for Spatial Data Interpolation of a Large Groundwater Quality Dataset from the Western Netherlands. Water (Switzerland), 16(18), 2581. doi:10.3390/w16182581.

[21] Al-Mamoori, S. K., Al-Maliki, L. A., Al-Sulttani, A. H., El-Tawil, K., & Al-Ansari, N. (2021). Statistical analysis of the best GIS interpolation method for bearing capacity estimation in An-Najaf City, Iraq. Environmental Earth Sciences, 80(20), 683. doi:10.1007/s12665-021-09971-2.

[22] Al-Maliki, L. A. J., Al-Mamoori, S. K., El-Tawel, K., Hussain, H. M., Al-Ansari, N., & Jawad Al Ali, M. (2018). Bearing Capacity Map for An-Najaf and Kufa Cities Using GIS. Engineering, 10(05), 262–269. doi:10.4236/eng.2018.105018.

[23] ASTM D4318-05. (2010). Standard Test Methods for Liquid Limit, Plastic Limit, and Plasticity Index of Soils. ASTM International, Pennsylvania, United States. doi:10.1520/D4318-05.

[24] Qusai, A. H., Szendefy, J., & Vásárhelyi, B. (2025). Effect of Changing Sand Content on Liquid Limit and Plasticity Index of Clay. Geotechnics, 5(1), 4. doi:10.3390/geotechnics5010004.

[25] Snethen, D. R. (1979). Technical guidelines for expansive soils in highway subgrades. Final Report, No. FHWA-RD-79-51, Engineering Research and Development Bureau, Washington, United States.

[26] Asuri, S., & Keshavamurthy, P. (2016). Expansive Soil Characterisation: an Appraisal. INAE Letters, 1(1), 29–33. doi:10.1007/s41403-016-0001-9.

[27] Casagrande, A. (1948). Classification and Identification of Soils. Transactions of the American Society of Civil Engineers, 113(1), 901–930. doi:10.1061/taceat.0006109.

[28] Chen, F. H. (2012). Foundations on expansive soils. Elsevier, Amsterdam, Netherlands.

[29] Holtz, W. G., & Gibbs, H. J. (1956). Engineering Properties of Expansive Clays. Transactions of the American Society of Civil Engineers, 121(1), 641–663. doi:10.1061/taceat.0007325.

[30] Samsonova, V. P., Blagoveshchenskii, Y. N., & Meshalkina, Y. L. (2017). Use of empirical Bayesian kriging for revealing heterogeneities in the distribution of organic carbon on agricultural lands. Eurasian Soil Science, 50(3), 305–311. doi:10.1134/S1064229317030103.

[31] Davila Saavedra, L., & Deutsch, C. V. (2025). Automatic variogram calculation and modeling. Computers and Geosciences, 195, 105774. doi:10.1016/j.cageo.2024.105774.